# Distribution of type I $Fc_\epsilon$-receptors on the surface of mast cells probed by fluorescence resonance energy transfer

Ulrich Kubitscheck,* Reinhard Schweitzer-Stenner,* Donna J. Arndt-Jovin,‡ Thomas M. Jovin,‡ and Israel Pecht§

*Institute of Experimental Physics, University of Bremen, W-2800 Bremen 33, Germany; ‡Department of Molecular Biology, Max Planck Institute for Biophysical Chemistry, W-3400 Göttingen, Germany; and §Department of Chemical Immunology, Weizmann Institute of Science, Rehovot 76100, Israel

ABSTRACT The aggregation state of type I $Fc_\epsilon$-receptors ($Fc_\epsilon RI$) on the surface of single living mast cells was investigated by resonance fluorescence energy transfer. Derivatization of $Fc_\epsilon RI$ specific ligands, i.e., immunoglobulin E or Fab fragments of a $Fc_\epsilon RI$ specific monoclonal antibody, with donor and acceptor fluorophores provided a means for measuring receptor clustering through energy transfer between the receptor probes. The efficiency of energy transfer between the ligands carrying distinct fluorophores was determined on single cells in a microscope by analyzing the photobleaching kinetics of the donor fluorophore in the presence and absence of receptor ligands labeled with acceptor fluorophores. To rationalize the energy transfer data, we developed a theoretical model describing the dependence of the energy transfer efficiency on the geometry of the fluorescently labeled macromolecular ligands and their aggregation state on the cell surface. To this end, the transfer process was numerically calculated first for one pair and then for an ensemble of $Fc_\epsilon RI$ bound ligands on the cell surface. The model stipulates that the aggregation state of the $Fc_\epsilon RI$ is governed by an attractive lipid-protein mediated interaction potential. The corresponding pair-distribution function characterizes the spatial distribution of the ensemble. Using this approach, the energy transfer efficiency of the ensemble was calculated for different degrees of receptor aggregation. Comparison of the theoretical modeling results with the experimental energy transfer data clearly suggests that the $Fc_\epsilon RI$ are monovalent, randomly distributed plasma membrane proteins. The method provides a novel approach for determining the aggregation state of cell surface components.

## INTRODUCTION

Clustering of the cell surface type 1 receptor for $Fc_\epsilon$ ($Fc_\epsilon RI$)[1] domains of immunoglobulin E (IgE) on mast cells and basophils initiates a cascade of reactions culminating in secretion of mediators of inflammation (Siraganian, 1988). This system is of intrinsic interest and also provides a useful model for studying the common process of signaling across cell membranes induced by receptor clustering (Gill et al., 1987; Yarden and Ullrich, 1988).

$Fc_\epsilon RI$ aggregation can be accomplished via cross-linking of bound IgE by specific antigens or directly by $Fc_\epsilon RI$ specific antibodies (Ortega et al., 1988). However, it is still unclear what physical and steric requirements must be met by the receptor aggregates to effect the cellular response (Metzger et al., 1986). The search for a physical definition in terms of cluster size, flexibility, geometry, and lifetime of the receptor aggregates is a current topic of considerable interest and active investigation (Erickson et al., 1986, 1991; Kane et al., 1988; Schweitzer-Stenner et al., 1987; Ortega et al., 1988; Pecht et al., 1991).

The extent and time course of the clustering process as caused by the receptor cross-linking is modulated by the valency and association state of the receptors in the resting state. Defining these properties of the $Fc_\epsilon RI$ was the objective of several experimental studies (Sullivan et al., 1971; Mendoza and Metzger, 1976; Schlessinger et al., 1976; McCloskey et al., 1984; Zidovetzki et al., 1986; Myers et al., 1992). The general conclusion of these studies was that the $Fc_\epsilon RI$ is monovalent and randomly dispersed on the surface of the cells. However, a critical examination of the cited literature reveals that the aggregation state of the receptor had not been defined inasmuch as the conclusions were based on mobility studies of the $Fc_\epsilon RI$ and, therefore, restricted to mobile receptors. Moreover, the above-mentioned studies also detected a considerable fraction of immobile receptors (25–50%) (see also Ryan et al., 1988). The aggregation state of these immobile receptors could not be determined.

We have investigated the $Fc_\epsilon RI$ aggregation state on the membrane of mucosal mast cells (line RBL-2H3) by a different method: fluorescence resonance energy transfer (FRET), a technique widely used to study protein aggregation (Veatch and Stryer, 1977; Chan et al., 1979; Sims, 1984; Fagan and Dewey, 1986; Hasselbacher et al., 1984). Since the extent of energy transfer depends on the inverse sixth power of the distance between donor and acceptor fluorophors, the method is very sensitive to small changes in the aggregation state of appropriately labeled proteins in the plasma membrane. It is not straightforward, however, to extract information concerning the state of aggregation from the data if the components in question are densely distributed on the

Present address of Ulrich Kubitscheck: Department of Medical Physics and Biophysics, Robert-Koch-Str. 31, Westfälische Wilhelms Universität Münster, W-4400 Münster, Germany.

Address correspondence to Dr. Schweitzer-Stenner.

[1] *Abbreviations used in this paper:* $Fc_\epsilon RI$, type I $Fc_\epsilon$-receptor; FITC, fluorescein-5-isothiocyanate; FRET, fluorescence resonance energy transfer; IgE, immunoglobulin E; PBS, phosphate buffered saline; TRITC, tetramethylrhodamine isothiocyanate.



0006-3495/93/01/110/11 $2.00

cell surface. In this case, energy transfer will occur for aggregated as well as for randomly distributed proteins. Hence, a correct interpretation of the energy transfer data requires comparison of the results with a detailed model description of the experimental situation. In the first part of this report, we present such a model and subsequently compare it with experimental results.

A new method has recently been introduced to measure energy transfer between cellular components on single cells under the microscope in which the rate of donor photobleaching is related to the energy transfer efficiency (Jovin and Arndt-Jovin, 1989*a, b*). The advantages of this technique, denoted photobleaching FRET, have been discussed and its feasibility established in a number of experimental studies (Jovin and Arndt-Jovin, 1989*a, b;* Kubitscheck et al., 1991). The method avoids the major problems of measuring energy transfer by sensitized emission, namely errors due to light scattering, photobleaching of the fluorescent probes during data acquisition, and lack of registration of multiple images. Data of sufficient statistical significance can be accumulated by multiple repetitions of the measurements. We have applied photobleaching FRET in a study of donor and acceptor labeled $Fc_\epsilon RI$ bound ligands on single living mast cells.

In the following, we begin with a brief review of energy transfer theory and then describe a simple geometrical model for fluorescently conjugated macromolecular ligands bound to cell surface receptors. This geometrical model is used to calculate the FRET efficiency between a pair of donor and acceptor labeled ligands as a function of their separation. In the calculation, we consider two extreme cases of dye distribution on the receptor ligands. In the first, a strictly surface labeling of the ligand is assumed, whereas in the second case the distribution of dye on the ligand is taken to be spatially homogenous.

In the second step of the analysis, we calculate the spatial distribution of an ensemble of molecules on a cell surface by means of their pair-distribution function (Perelson, 1978). We assume an attractive lipid-mediated protein–protein interaction potential, $u(r)$, with different binding energies (Pearson et al., 1984) that lead to different extents of receptor aggregation. The pair-distribution functions are calculated by an iterative numerical procedure according to the approach of Pearson et al. (1983).

Third, the results of the first two steps are combined and we obtain predictions of the energy transfer efficiency for an ensemble of ligands bound to cell surface receptors. We modeled two different ligands for the $Fc_\epsilon RI$, a monovalent Fab-fragment of a IgG class monoclonal $Fc_\epsilon RI$-specific antibody (H10-Fab) (Ortega et al., 1988) and an intact monoclonal IgE molecule secreted by the hybridoma clone A2 (Rudolph et al., 1981), also monovalent for $Fc_\epsilon RI$. The predicted ratios of the energy transfer efficiencies of the probes are calculated as a function of their surface density at different degrees of receptor aggregation and compared with the experimental results.

## THEORY

### FRET

A fluorophore decays from its excited state at a rate $k_d$ by radiative and nonradiative processes. If nonradiative energy transfer takes place to a suitable acceptor with rate $k_{et}$, the new decay rate $k'_d$ is given by

$$k'_d = k_d + k_{et}. \tag{1}$$

Förster (1948) showed that

$$k_{et} = k_d \cdot (R_0/r)^6, \tag{2}$$

where $r$ is the distance between the donor and the acceptor. $R_0$, the so-called Förster distance for 50% transfer, is a constant specific for any given donor-acceptor pair. It is a function of the refractive index of the medium, the quantum yield of the donor in absence of the acceptor, the orientation between the absorption and emission transition dipole moments of the acceptor and donor molecules, respectively, and the overlap integral of the donor emission and the acceptor absorption spectra. The energy transfer efficiency $E$ is defined by

$$E = k_{et}/(k_{et} + k_d), \tag{3}$$

and from Eq. 2 is 0.5 for $r = R_0$. Fluorophores in the excited state may also be photobleached, i.e., they undergo irreversible photochemical decomposition. The probability of photobleaching depends on the excited state lifetime. As a consequence, any process that reduces the lifetime (such as energy transfer) will result in a slower rate of photobleaching. Thus, the photobleaching time constant is increased in the case of energy transfer ($\tau'$) compared with that of the same system without energy transfer ($\tau$), i.e., in the absence of an acceptor. Jovin and Arndt-Jovin (1989*a*) showed that the energy transfer efficiency $E$ is a function of the photobleaching time constants $\tau'$ and $\tau$ according to:

$$E = 1 - \tau/\tau'. \tag{4}$$

This equation is correct for donor molecules with uniform photobleaching kinetics, i.e., $\tau$. In an experimental situation, however, there may be distributions of the donor photobleaching rates due to structural heterogeneities, variable donor-acceptor geometry, and varying access to oxygen molecules. In a previous article (Kubitscheck et al., 1991), we asserted that the photobleaching of an ensemble of donors with a rectangular distribution of photobleaching rate constants $k_{bl}$, such that $k_{bl} \in [k_{low}, k_{high}]$ and $k_{high} < 5 \cdot k_{low}$, can still be described by a monoexponential decay with an effective rate constant $k_{eff} = 1/\tau_{eff}$, where $k_{eff} \approx (k_{high} - k_{low})/2$. If the total distribution is shifted to lower rates by a factor $1\text{-}E$ due

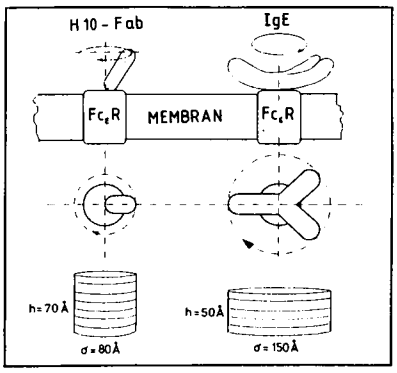


FIGURE 1 Hypothetic binding configurations of IgE and H10-Fab. The upper part of the figure shows side views of H10-Fab and IgE molecules bound to Fc$_\epsilon$RI. The H10-Fab is assumed to bind in an approximately perpendicular orientation with respect to the cell surface. The IgE molecule is bound parallel to but tilted away from the cell surface (Holowka and colleagues, 1983, 1985; Zheng et al., 1991). The central section shows topviews. We approximate the bound ligands as cylinders of the given geometries.

to FRET, a second effective rate constant $k'_{\text{eff}} = 1/\tau'_{\text{eff}}$ can be determined, in accordance with the expression

$$E \approx 1 - \tau_{\text{eff}}/\tau'_{\text{eff}}. \tag{5}$$

Hence, the energy transfer efficiency $E$ can be obtained by measuring the photobleaching of donor fluorophores in the presence and absence of acceptor molecules regardless of heterogeneities in the system, if the decay curve can effectively be described by a monoexponential function.

## Energy transfer between cell surface receptor bound ligands

### Fluorescently labeled ligands approximated as cylinders

To estimate the energy transfer efficiency between antibodies bound to cell components, we need a geometrical model for these complexes. Fig. 1 schematically shows the binding configurations of an Fc$_\epsilon$RI specific Fab and of an IgE molecule bound to the Fc$_\epsilon$RI. We assume that the Fab-fragment binds with some angle between its long axis and the normal to the cell surface. The binding configuration of the IgE molecule is sketched according to the results of Holowka and Baird (1983), Holowka et al. (1985), and Zheng et al. (1992). We approximate the shape of the bound molecules by cylinders, the main axes of which are perpendicular to the plane of the membrane (Fig. 1). This is the simplest model for the binding geometry that retains the main features of the system, namely that the IgE molecule is longer and larger than the Fab molecule.

### Energy transfer between two cylinders on a surface

Isothiocyanates of fluorescein (FITC) and tetramethylrhodamine (TRITC) are the donor and acceptor dyes utilized for labeling the receptor ligands. They were covalently conjugated to amino groups of the proteins. In an approximation to the real situation, we describe the labeling of the derived models by a constant dye density on the surface of the cylinders. This density is determined by the size of the ligand and the dye/protein ratio.

The efficiency of energy transfer between cylinders with constant donor and acceptor surface densities must be calculated numerically. For that purpose, we divide the cylinder envelope into a number of equally sized subsurfaces, each with an equal probability of carrying a fluorophore. The efficiency $E_i$ for energy transfer between a single donor i and $N_a$ acceptors is given by Dewey and Hammes (1980)

$$E_i = 1 - \left[1 + \sum_{j=1}^{N_a} (R_0/r_{ij})^6\right]^{-1}, \tag{6}$$

where $r_{ij}$ is the distance between donor i and acceptor j. The total efficiency $E_s$ of energy transfer between $N_d$ donors and $N_a$ acceptors is obtained by averaging over all donor contributions according to Dewey and Hammes (1980):

$$E_s = 1/N_d \cdot \sum_{i=1}^{N_d} E_i. \tag{7}$$

The geometry of the cylinders is specified according to the binding configurations given in Fig. 1. The H10-Fab has a length of $\approx$80 Å (Edmundson and Ely, 1986); we assign to the corresponding cylinder a diameter $\sigma$ = 80 Å and a height $h$ = 70 Å (see Fig. 1). An IgE molecule has a length of $\approx$180 Å (Holowka and Baird, 1983). Due to its proposed bent configuration on the cell surface, we assume that the respective cylinder (Fig. 1) has a diameter $\sigma$ = 150 Å and a height $h$ = 50 Å. A recent study by FRET (Zheng et al., 1992) of the conformation of Fc$_\epsilon$RI bound IgE extends the former results of Holowka and Baird and proposes a strong bend of the IgE molecules with a distance of $\approx$70 Å between the COOH-terminus and the antigen binding sites. A rotation of such a bent IgE molecule, however, produces a cylinder with dimensions close to the above values, which thus seem reasonable if one disregards the conformational details. $E_s$ was numerically calculated as a function of the separating distance $d$ between donor and acceptor cylinders; $d$ is defined as the distance between the projections of the centers of mass of the cylinders onto the cell surface.

The results of the numerical calculations are presented in Fig. 2 in which $E_s$ is displayed as a function of $d$ for IgE- and H10-cylinders considering two different values of dye concentration on the acceptor cylinder (H10: $n_a$ = 1.3 and 1.5, IgE: $n_a$ = 4 and 11). These values were derived from our experimentally determined dye/protein ratios of different preparations. $E_s$ is independent of the dye concentration in the donor cylinder. We assumed that the cylinders cannot interpenetrate, and thus calculated $E_s(d)$ only for distances larger than the cylinder

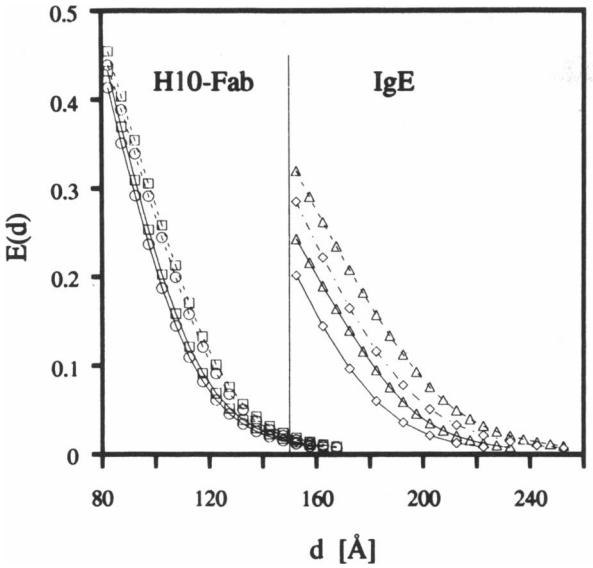


FIGURE 2 Fluorescence resonance energy transfer efficiency $E(d)$ as a function of the distance $d$ between two cylinders assuming a homogeneous dye distribution on the envelope surface (*dashed lines*) or inside (*solid lines*) of the cylinders. The energy transfer efficiency $E(d)$ was numerically calculated for the cylinders sketched in Fig. 1 (H10-Fab: $\sigma$ = 80 Å, $h$ = 70 Å; IgE: $\sigma$ = 150 Å, $h$ = 50 Å). Number of dye labels in the acceptor cylinder: H10-Fab: $n_a$ = 1.3 (○) and 1.5 (□); IgE: $n_a$ = 4 (◇) and 11 (△); Förster distance $R_0$ = 63 Å (Chan et al., 1979).

diameter. As shown in Fig. 2 *A*, $E_s(d)$ at direct contact of the cylinders ($d = \sigma$) is larger for the H10-Fab ($E_s(\sigma)$ = 0.44 and 0.45 for $n_a$ = 1.3 and 1.5, respectively) than for the more extensively labeled IgE ($E_s(\sigma)$ = 0.28 and 0.32 for $n_a$ = 4 and 11, respectively). The slope describing the decrease of the energy transfer efficiency with distance, however, is steeper for the H10-Fab than for the IgE cylinders.

To assess the influence of the dye distribution on the results of the above calculations, we considered a second completely different limiting case: a constant volume density of the donor and acceptor dyes in the cylinders. Using the above numerical approach with the respective parameters, we again calculated the distance dependence of the FRET efficiency for a pair of donor-acceptor cylinders. The results of this model are given by the solid lines in Fig. 2. As for the first model, the FRET is again more efficient for cylinders in direct contact when using the H10-Fabs ($E_s(\sigma)$ = 0.41 and 0.42 for $n_a$ = 1.3 and 1.5, respectively) but decreases faster with distance than for IgE molecules that exhibit a lower transfer efficiency on contact ($E_s(\sigma)$ = 0.20 and 0.24 for $n_a$ = 4 and 11, respectively).

Thus, for the two extreme cases of dye distribution, in or on the macromolecular ligands, we predict that H10-Fabs should show a higher energy transfer at small distances and IgEs at larger distances. This important result is a consequence of the smaller dimensions of the H10-Fab compared with the IgE and hence constitutes a general feature of the system.

### Cell surface distribution of membrane proteins

Using the geometrical model described above for the macromolecular ligand-receptor complexes, the energy transfer efficiency is now calculated for ensembles of ligands (here bound to $Fc_\epsilon RI$) on a surface. We consider the distance distribution of receptors for different interaction potentials that produce an increasing receptor aggregation. For these different cases, we finally calculate the overall energy transfer efficiency for ensembles of receptor bound H10-Fab or IgE on whole cells.

The distance distribution of particles is determined by their pair-distribution function $g(r)$ (McQuarrie, 1976). Choosing an arbitrary central particle with a radial symmetrical interaction potential, the average number $n(r)dr$ of particles located in a shell of radius $r$, $r + dr$ is given by

$$n(r)dr = \rho g(r) 2\pi r dr, \qquad (8)$$

where $\rho$ is the surface density of the particles. In principle, $g(r)$ depends on the nature of all existing receptor–receptor and receptor–lipid interactions.

We assume that the receptor-bound ligands are cylindrical with a diameter $\sigma$ and cannot interpenetrate, i.e., the potential $u(r) = \infty$ for $r \leq \sigma$. Although the sketch in Fig. 1 suggests that interpenetration of two colliding liganded receptors should be possible, we introduce this assumption for two reasons. (*a*) The rotational diffusion of the receptors occurs on the same time scale as the translational diffusion, thus hindering approaches closer than the outer radii of the respective entities. (*b*) We are not aware of any experimental studies that could contribute to a more realistic model of the close range interaction between membrane proteins.

We assume further that attractive forces between the receptors may be caused by a lipid-mediated protein–protein interaction potential. The physical basis of this potential is the distortion of the protein-free equilibrium configuration of the membrane due to the presence of proteins, which raises the energy of a bilayer containing membrane proteins compared with one lacking them. This potential has been analyzed in detail by Pearson and co-workers (1984), and we describe $u(r)$ for $r > \sigma$ by Eq. 17 of their work. The potential is characterized by a correlation length and an interaction energy $E_{int}$. A larger interaction energy would naturally cause an increase in receptor association. We consider interaction energies $E_{int}$ between 0 and 1.5 $kT$, where $k$ designates the Boltzmann constant and $T$ the absolute temperature. Such interaction energies correspond to binding energies of up to 3.75 kJ mol$^{-1}$ at room temperature. Hence, their strength is assumed to be equivalent to that of several combined van der Waals bonds (0.2–0.5 kJ mol$^{-1}$) but is significantly smaller than that of hydrogen bonds or ion bonds (10–30 kJ mol$^{-1}$).

The complete potential $u(r)$ utilized in our simulation is shown in Fig. 3. The distances are normalized to the receptor diameter, i.e., $r_{red} = r/\sigma_{Fc_\epsilon RI}$. The potential en-

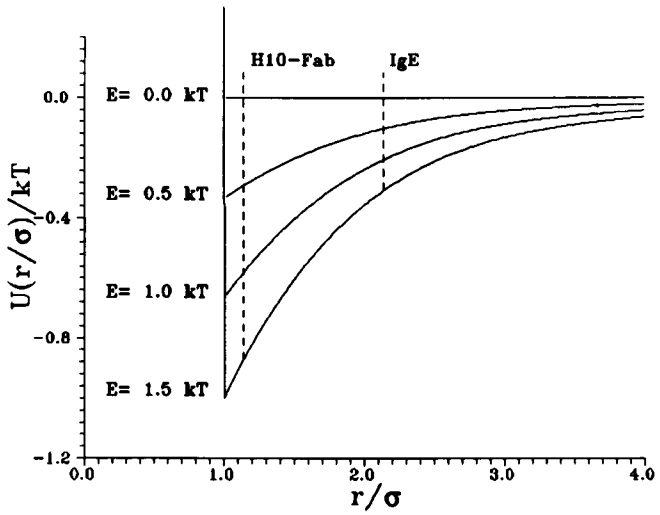


FIGURE 3 Lipid-mediated protein–protein interaction potential $u(r)$ as a function of reduced radius $r/\sigma$ ($\sigma$: diameter of the $Fc_\epsilon RI$) with a correlation length of $2\sigma$ and different interaction energies as indicated (and according to Fig. 3 of Pearson et al., 1984). The dashed lines indicate the diameters of the H10-Fab and IgE cylinders compared with the diameter of the $Fc_\epsilon RI$. To the right of these dashed lines are the regions of the potentials sensed by the respectively liganded $Fc_\epsilon RI$.

ergy function exhibits a minimum at distances just larger than the particle diameter, corresponding to $r/\sigma = 1$. For $r/\sigma > 1$, the function increases slowly to zero. The radial range of the attractive forces caused by this potential is characterized by the correlation length that we assume to be equal to $2\sigma_{Fc_\epsilon RI}$, a value that is in the range of experimental results for membrane proteins (Pearson et al., 1984). The dashed lines indicate the diameters of the H10-Fab and IgE liganded $Fc_\epsilon RI$ cylinders in comparison with the diameter of the free $Fc_\epsilon RI$. On the right-hand side of these dashed lines, the regions represent the potentials sensed by the respectively liganded $Fc_\epsilon RI$ as discussed in more detail below.

To calculate the pair-distribution functions that correspond to this model, we use a modification of the methodology of Pearson et al. (1984) based on an algorithm of Lado (1968). The pair distribution function, $g(r)$, is calculated using the Ornstein-Zernike equation

$$h(r) = c(r) + \rho \int c(|\mathbf{r} - \mathbf{s}|)h(|\mathbf{s}|)\, d^2s, \qquad (9)$$

where $h(r)$ is the indirect correlation function, defined as $h(r) = g(r) - 1$, and $c(r)$ is the direct correlation function. The integration is carried out in two dimensions extending from $-\infty$ to $+\infty$; $s$ is a dummy integration variable. The bold print style indicates a vector on the surface plane. The approximate Percus-Yevick equation for $c(r)$ (Pearson et al., 1984),

$$c(r) = g(r)\{1 - e^{u(r)/kT}\}, \qquad (10)$$

completes the set of equations. The Ornstein-Zernike equation is of convolution type and can be deconvoluted by a two-dimensional Fourier transform. The latter reduces to the Hankel transform, a one-dimensional transform with a Bessel function kernel, due to the radial symmetry of $h(r)$. Thus,

$$\hat{h}(k) = \hat{c}(k)/[1 - \rho\hat{c}(k)], \qquad (11a)$$

$$\hat{c}(k) = \hat{h}(k)/[1 + \rho\hat{h}(k)], \qquad (11b)$$

where $k$ is a scalar variable in frequency space. The solution of these equations is effected by an iteration procedure. Starting with a guess for $c(r)$, the Hankel transform $\hat{c}(k)$,

$$\hat{c}(k) = 2\pi \int_0^\infty c(r)J_0(kr)r\, dr, \qquad (12)$$

is calculated numerically and used in Eq. 11a to obtain the Hankel transform of $h(r)$, i.e., $\hat{h}(k)$. This function is then transformed to $h(r)$, which is corrected for $r \leq \sigma$ for which $h(r) = -1$. The corrected $h(r)$ is transformed to frequency space, and a second approximation of $\hat{c}(k)$ is calculated from Eq. 11b. This improved $\hat{c}(k)$ is transformed to $c(r)$ and corrected by the Percus-Yevick relation for $r > \sigma$. The procedure is iterated until the changes in subsequent approximations of $g(r)$ are $<10^{-3}$.

The particle density $\rho$ of the $Fc_\epsilon RI$ on RBL-2H3 cells is estimated to be $800 \pm 500\ \mu m^{-2}$ (Kubitscheck, 1990). The relevant specific volume of the $Fc_\epsilon RI$ is probably limited to that of the extracellular domains, i.e., the two Ig-like domains of the $\alpha$-subunit that can be approximated in volume by the variable domains of antibodies (Blank et al., 1989). Assuming that these domains lie parallel to the membrane, the maximal diameter is ~70 Å. To simplify the numerical computations for the pair distribution function, dimensionless variables are introduced by using a reduced length scale ($r_{red} = r/\sigma$) with the respective cylinder diameter as unit length. Consequently, the differing diameters $\sigma$ of the $Fc_\epsilon RI$-bound H10-Fab or IgE yield different values for the respective reduced density $\rho\sigma^2$. The latter is considerably higher for the IgE-$Fc_\epsilon RI$ complex than for that of H10-Fab-$Fc_\epsilon RI$ or for the free $Fc_\epsilon RI$. For example, with $\rho = 800\ \mu m^{-2}$, reduced densities are 0.04 for $Fc_\epsilon RI$ cylinders, 0.051 for H10-Fab, and 0.18 for IgE cylinders. Due to the difficulty in determining cell surface area and to variations in the receptor number from cell to cell, there is a considerable uncertainty associated with the estimation of the surface density $\rho$. Thus, we calculated the necessary correlation functions for densities in an appropriate range, i.e., from 0.015 up to 0.064 for the $Fc_\epsilon RI$ cylinders and corresponding values for the respective ligand-receptor complexes.

The diameters of the H10 and IgE cylinders exceed that of the $Fc_\epsilon RI$ cylinder. Hence, these receptor-ligand complexes probe different regions of the interaction potential than the free receptors in the lipid bilayer. For example, the H10-Fab labeled receptors can approach each other more closely than the more sterically hindered IgE labeled receptors. Thus, given a distance de-

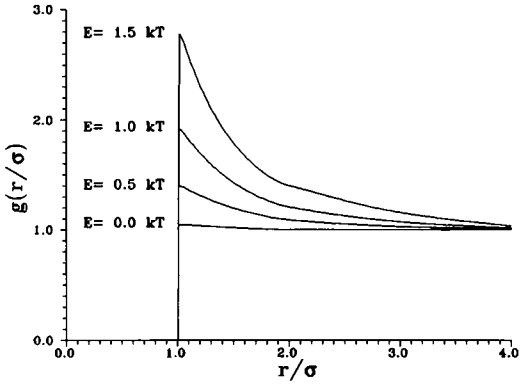


FIGURE 4 Pair distribution function $g(r/\sigma)$ of Fc$_\epsilon$RI (approximated as cylindrical particles of 70 Å) at a reduced density $\rho\sigma^2$ of 0.04 as function of $r/\sigma$. $g(r/\sigma)$ was calculated according to the numerical algorithm using Eqs. 9–12 and the interaction potential given in Fig. 3. Binding energies were assumed as indicated. The maximal increase with the interaction energies, demonstrating a growing extent of aggregation. $g(r/\sigma) = 0$ for $r/\sigma < 1$ since the cylinders are not allowed to interpenetrate.

pendent attractive interaction, H10-Fab bound receptors may be more extensively aggregated than IgE labeled receptors. This size effect was considered in the numerical computations yielding the pair-distribution functions by using different regions of the interaction potential for the two different receptor ligands, as indicated in Fig. 3. The phenomenon would occur for all possible different interaction potentials and hence is another general feature of the system.

We used the above algorithm to calculate the pair-distribution functions for the Fc$_\epsilon$RI, the H10-Fab, and the IgE cylinders for different surface densities and binding energies. As an example, results of the calculations for the Fc$_\epsilon$RI cylinders at the reduced density $\rho\sigma^2 = 0.04$ and different binding energies $E_{int}$ between 0 and 1.5 kT are shown in Fig. 4. Since we used a hard core potential, $g(r)$ is zero for $r \leq \sigma$. The attractive potential causes the maximum in the function near $r = \sigma$. The increase in the height of the maximum for increasing binding energies indicates a growing particle aggregation. To estimate the amount of aggregation in these cases, we define cylinders having a distance of ~5 Å or less to each other (approximately the length of a van der Waals bond) as aggregated. This yielded that 2, 3, 4, and 6% of the particles were aggregated assuming a binding energy of 0, 0.5, 1, and 1.5 kT, respectively. In other words, even in the absence of binding energy (0 kT), a certain number of receptors are aggregated as a consequence of random encounters of Fc$_\epsilon$RI; $g(r)$ approaches unity for large $r$, for which the correlations caused by the interaction potential vanish.

### Energy transfer in an ensemble of receptor ligands

We now consider the total efficiency of energy transfer $E_{ens}$ in an ensemble of cylindrical particles on a two-dimensional surface. The particles are labeled by fluorescent donors and acceptors, respectively, at a ratio of 1:1. The energy transfer efficiency $E_s(r_{ij})$ for a single donor-acceptor cylinder pair (i, j) as a function of the distance $r_{ij}$ was calculated numerically as discussed above, and the result for our specific model is given in Fig. 2. Furthermore, we already determined the pair-distribution function $g(r)$, describing the average number of acceptor cylinders in a shell of radius $r$, $r + dr$ around a central donor cylinder for the respective interaction potentials, cylinder geometries, and particle densities.

Each donor cylinder i encounters $m_{i,r_c}$ acceptor cylinders located at distances $r_{ij}$ (j = 1, 2, . . . , $m_{i,r_c}$) within a circle of radius $r_c$. Here, the average number $m_{ave,r_c}$ of encountered acceptors is found by integration of Eq. 8 from $r = 0$ to $r = r_c$. Thus, the individual $m_{i,r_c}$ (and hence $r_{ij}$) follow the respective probability distribution. All these acceptors j contribute an energy transfer efficiency $E_s(r_{ij})$ to the total energy transfer efficiency $E_i$ of each donor i, which is calculated by summation over all acceptors according to Eq. 6. Here, however, not the distances $r_{ij}$ must be used, but rather "effective" distances $r'_{ij}$. The latter are defined as the distances by which the dye molecules of i, located at a single point, must be separated from the dye molecules of j, located at another point, to yield an energy transfer efficiency $E_s(r_{ij})$:

$$r'_{ij} = R_0 \sqrt[6]{[1 - E_s(r_{ij})]/E_s(r_{ij})}, \qquad (13)$$

where $E_s(r_{ij})$ corresponds to the energy transfer efficiency of the donor and acceptor cylinders as shown in Fig. 2. Finally, the contributions of all donors $E_i$ must be averaged according to Eq. 7, yielding the complete energy transfer $E_{ens}$ of the ensemble.

The approach outlined above to calculate $E_{ens}$ was realized by means of a Monte Carlo simulation. Using a pseudo random number generator, the distances $r_{ij}$ between donor i and its acceptors j were determined according to the particle distribution (cf. Eq. 8). Theoretically, the $r_{ij}$ for all acceptors j have to be determined. Most of them, however, will be located at distances from the donor much larger than the Förster radius, such that their energy transfer efficiency contribution is neglegibly small. Hence, in the computer simulation, we used the following procedure. First, we calculated the radii $r_n$ of circles around the donor cylinders, inside which $n$ acceptor particles are located, by integrating Eq. 8:

$$n = \int_0^{r_n} \rho g(r) 2\pi r \, dr. \qquad (14)$$

From this expression, $r_n$ was determined for $1 \leq n \leq 5$. Then, the distances of $n$ acceptor particles j from a donor particle i were determined by the Monte Carlo routine according to the respective pair distribution function ($r_{ij} \leq r_n$), and the energy transfer efficiency $E_i$ was calculated, as described above. This was repeated for $10^4$ donor cylinders i. Finally, $E_{ens}$ was calculated by averaging

$E_i$ according to Eq. 7. We found that already using three acceptors and hence $r_3$ as maximal distance, the ensemble energy transfer efficiency converged even for the highest particle density ($\Delta E_{ens}/E_{ens} < 0.01$ for 3 or more acceptor cylinders)

Thus, for all subsequent computations, we first determined $r_3$ and then located three acceptor particles j around the donor particles i using an average particle density according to Eq. 8. This was repeated for $2 \cdot 10^4$ donors, and finally their energy transfer contributions were averaged according to Eq. 7. The parameters of these Monte Carlo computations were the geometric dimensions of the cylinders, the particle surface density, $\rho$, the interaction potential, $u(r)$, the number of acceptor dyes per protein, $n_a$, and the Förster distance, $R_0$. Fig. 5, *A–D*, shows $E_{ens}$ as a function of the reduced density $\rho\sigma^2$ for the H10-Fab ($n_a = 1.5$) and IgE ($n_a = 11$), assuming the interaction potentials discussed above, a homogeneous dye distribution (*i*) on the surface or (*ii*) inside the cylinders and a Förster distance $R_0$ of 63 Å (Chan et al., 1979). The vertical displacement between the curves for the different binding energies demonstrates that the smaller size of the H10-Fab cylinders enhances and the larger size of IgE cylinders diminishes the influence of the attractive potential on the energy transfer efficiency of the labeled receptor ensemble. This feature is obtained for both models of the dye distribution. Corresponding results were derived for different numbers of acceptor dye molecules within or on the surface of the acceptor cylinders according to the respective experimental conditions (H10-Fab: $n_a = 1.3$, IgE: $n_a = 4$; data not shown).

The limited knowledge about cell surface morphology and thus receptor density also limits the direct comparison between the theoretical model and the experimental results. A solution to this problem is found by noting that the ratio of the efficiency of energy transfer for cylinders of largely differing size, as in the case of H10-Fab and IgE labeled receptors, is almost independent of the receptor density. Fig. 6, *A* and *B*, shows the calculated ratios $r_E = E_{IgE}/E_{H10}$ as a function of the receptor density for the indicated values of $n_a$ and binding energies. It can be concluded that the ratios are almost independent of the assumed dye distribution and receptor density and hence can be readily compared with the respective experimental results. The graphs are shown for the different labeling ratios of H10 and IgE. They suggest that high $r_E$ values (>1) must be related to a low or even zero attractive force between receptors, whereas low ratios $r_E$ are due to aggregated receptors.

In our analysis, we tried to achieve a quantitative estimate of the effect of ligand size on the energy transfer efficiency between molecules located on a cell surface. The above conclusions were obtained after considering a model using specific geometries for the receptor-IgE or receptor-Fab complexes. It should be stressed, however, that these conclusions are a consequence of the basic feature of the experimental system: the different geometry of the $Fc_\epsilon RI$ ligands used, i.e., IgE molecules and H10-Fabs. According to our model, the larger size of the IgE molecule compared with the receptor has the effect of reducing the interactions leading to aggregation. This is reflected by the special radial distribution function and the underlying interaction potential used for the IgE cylinders. The smaller size of the H10-Fab labeled receptors (*a*) allows a closer contact between the receptors and (*b*) leads to a higher energy transfer efficiency if such a contact occurs. Thus, our model is of general character despite the specific geometric assumptions.

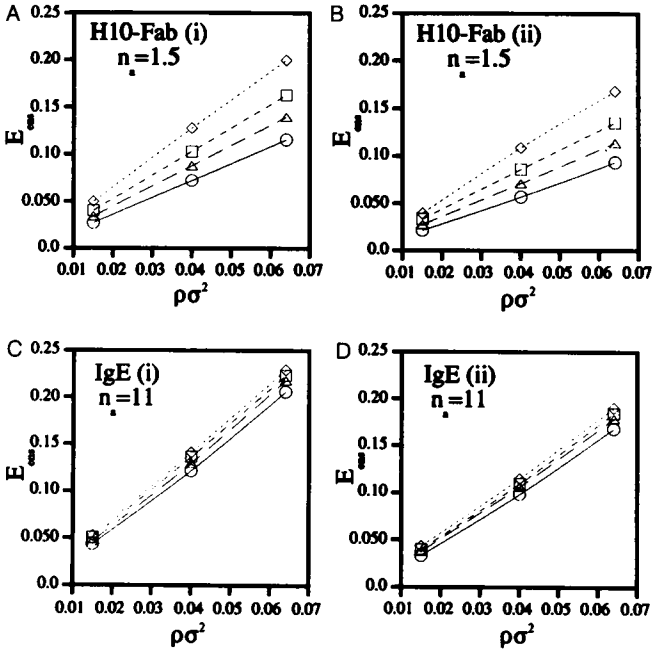


FIGURE 5 Ensemble fluorescence resonance energy transfer efficiency $E_{ens}$ as a function of the reduced cylinder particle density $\rho\sigma^2$ in dependence on the attractive interaction energy $E_{int}$. Calculations were performed using a Monte Carlo simulation as described in the text for the cylinder geometries of the H10-Fab (*A* and *B*) and IgE (*C* and *D*) molecules (see Fig. 1) and for the indicated numbers of dye molecules $n_a$ (i) on the envelope surface or (ii) inside the acceptor cylinder. The curves were calculated for different binding energies ($E = 0\,kT$[○], $0.5\,kT$[△], $1.0\,kT$[□], and $1.5\,kT$[◇]). The distance between the respective curves shows that the small size of the H10-Fab increases and the larger size of the IgE diminishes the effect of the attractive potential on the energy transfer efficiency.

## MATERIALS AND METHODS

### Cell culture

Rat mucosal mast cells, subclone 2H3 (RBL-2H3), were cultured at 37°C in Dulbecco's modified Eagle's medium containing 10% fetal calf serum (Barsumian et al., 1981).

### Fluorophore conjugation of the ligands

IgE (hybridoma line A2) and H10-Fab (Fab fragment derived from the $Fc_\epsilon RI$-specific IgG class mAb H10) were reacted with fluorescein isothiocyanate (FITC, isomer 1) or tetramethylrhodamine (TRITC,

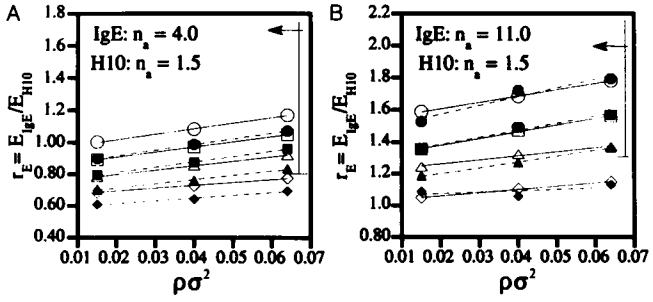


FIGURE 6 Ratio $r_E = E_{IgE}/E_{H10}$ of the calculated fluorescence resonance energy transfer efficiencies $E_{ens}$ (see Fig. 5) as a function of the reduced receptor density $\rho\sigma^2$. The stoichiometries of conjugated fluorophores are indicated for H10-Fab and IgE. Fluorophores were considered to lie either inside the acceptor cylinder (*closed symbols*) or on its envelope surface (*open symbols*). The curves calculated for different binding energies (symbols as in Fig. 5) show that high ratios $r_E$ are suggestive of weak or even the lack of attractive forces between receptors. Low ratios $r_E$ are indicative of aggregated receptors. The experimentally determined ratios for the respective cases (see arrows) are only compatible with the assumption of zero or very low interaction energies.

isomer 5), both dyes from Molecular Probes, Eugene, OR. Conjugation was performed in borate buffer at pH 9.4 as recently described by Kubitscheck et al. (1991). The A2-IgE and H10-IgG antibodies were characterized by Rudolph et al. (1981) and Ortega et al. (1988), respectively. The antibody concentration as well as the labeling ratios were determined by absorbance measurements using the following extinction coefficients: $\epsilon(IgE)_{280nm}$ = 300 $mM^{-1}$ $cm^{-1}$ (Liu et al., 1980); $\epsilon(FITC)_{280nm}$ = 27 $mM^{-1}$ $cm^{-1}$; $\epsilon(FITC)_{496nm}$ = 87 $mM^{-1}$ $cm^{-1}$; $\epsilon(H10\text{-}Fab)_{280nm}$ = 70 $mM^{-1}$ $cm^{-1}$ (Ortega et al., 1988); $\epsilon(TRITC)_{280nm}$ = 12.1 $mM^{-1}$ $cm^{-1}$; and $\epsilon(TRITC)_{556nm}$ = 23.1 $mM^{-1}$ $cm^{-1}$. The absorption coefficients of FITC and TRITC were determined from the absorbances of standard solutions.

## Cell sample preparation for energy transfer experiments

Microscope coverslips (12 mm diam) were washed successively in 3% acetic acid, 75% isopropanol, and bidistilled water and sterilized by autoclaving. RBL-2H3 cells were grown to subconfluence on the coverslips in DMEM, 10% FCS. Then coverslips were washed twice with PBS and incubated with 25 $\mu$l of 100 nM FITC-IgE or 100 nM FITC-H10-Fab in PBS for 45 min at room temperature for the singly labeled, i.e., only donor bound, samples. For the doubly labeled samples, i.e., cells with $Fc_\epsilon RI$ with both donor and acceptor carrying ligands, the coverslips were incubated with 25 $\mu$l of 50 nM FITC-IgE and 50 nM TRITC-IgE or 50 nM FITC-H10-Fab and 50 nM TRITC-H10-Fab in PBS. The coverslips were washed again in PBS before being mounted in a small temperature controlled Teflon chamber filled with PBS ($T$ = 25°C). Cells were allowed to equilibrate in the chamber for 10 min before starting the measurements.

## Photobleaching experiments on single cells

The experimental setup and the measuring procedure have been described in detail elsewhere (Kubitscheck et al., 1991). In short, cells attached to coverslips were reacted with the appropriate ligands as described and photobleached in a chamber mounted in an epi-illumination fluorescence microscope (Leitz MPV2; Ernst Leitz GmbH, Wetzlar, Germany). Fluorescein was excited by the 495.5-nm line of an Ar-laser (output power 15 mW). The MPV2 is equipped with an image aperture used to select single cells for measurements. The fluorescence from an examined cell was focused by a 95 × 1.32 objective and passed through a 500-nm dichroic mirror and a 5-nm half-width interference filter centered at 515 nm. The intensity was measured by an photon counting system and the data transferred online to a IBM compatible PC for display and analysis. Data fitting was performed using the $X^2$-minimization program MINUIT obtained from the CERN Program library (James, 1972).

## Fluorescence polarization measurements

Subconfluent RBL-2H3 cells were grown, released from the culture dishes, and labeled with FITC-IgE as described (Kubitscheck et al., 1991). The cells were kept in suspension on ice until they were transferred to a cuvette for fluorescence polarization measurements. The 496.5-nm line of an Argon laser (Spectra Physics GmbH, Darmstadt, Germany) was used for excitation and the parallel ($I_{||}$) and perpendicular polarized ($I_\perp$) fluorescence emission was registered at 520 nm (HW 3 nm) with a Czerny-Turner double monochromator (Spex GmbH, Munich, Germany) equipped with photon counting system (EG&G Ortec GmbH, Munich, Germany). The sample was illuminated with an unfocused laser beam (output power 0.2 mW) only during the recording of the fluorescence signal, i.e., 30 s. Under these conditions, the photobleaching of the FITC was negligible.

## RESULTS

We measured the time dependence of photobleaching fluorescein conjugated IgE-A2 or H10-Fab bound to adherent single RBL-2H3 cells in the absence (singly labeled cells) and in the presence (doubly labeled cells) of the corresponding acceptor (TRITC) conjugated macromolecular probe. In a previous study utilizing the photobleaching technique, FITC-conjugated monoclonal, DNP-specific IgE were used as donor and the binding DNP-haptens as acceptor probes (Kubitscheck et al., 1991). In contrast to this donor-acceptor pair, the acceptor of the present study is fluorescent as well. Thus, care must be taken to check for contributions of TRITC fluorescence to the donor bleaching signal. However, there was no background fluorescence produced by excitation of the TRITC-conjugated ligands. This was checked by comparing the fluorescence of unlabeled cells and TRITC conjugated IgE labeled cells. The fluorescence intensities and bleaching characteristics of both samples were identical (data not shown). Furthermore, visual inspection of the TRITC fluorescence of the cells (excitation 528 nm, emission above 560 nm) showed the common ring staining of cells. There were no spots of TRITC fluorescence indicative of aggregated ligands.

There is the possibility of energy self-transfer between donors on different IgE or H10-Fab molecules. Such a self-transfer was not considered in our theoretical description of the system. To examine this possibility experimentally, we performed measurements of the fluorescence polarization of singly labeled cell samples as a function of the number of IgE-FITC per cell. Energy self-transfer would lead to decreasing values of the fluorescence polarization for increasing numbers of donor

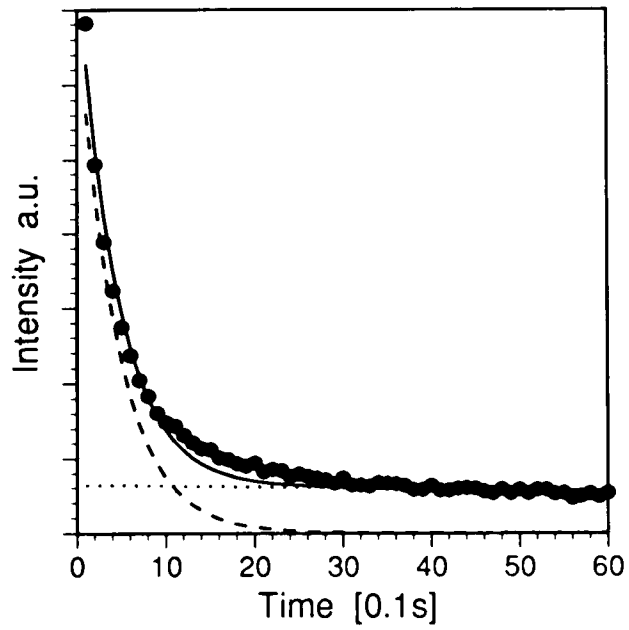


FIGURE 7 Fluorescence photobleaching of a single FITC-IgE labeled RBL-2H3 cell. The fluorescence intensity of RBL-2H3 cells carrying FITC labeled ligands was measured under conditions of strong laser illumination (496.5 nm, output power 15 mW) as a function of time (· · ·). The solid line is the result of a fitting process with two exponentials ($\tau_1$ = 0.6 s, $\tau_2$ = 25 s). The first component is due to fluorescein bleaching (- - -) and the second to the bleaching of the fluorescence background (· · ·), i.e., autofluorescence of the cell and optics.

probes on the cell surface. However, the fluorescence polarization ratio $r_p = I_{\parallel}/I_{\perp}$ of different samples from saturation down to 30% occupation of the $Fc_\epsilon RI$ with IgE-FITC was constant, and equal to $r_p = 1.9 \pm 0.1$. This indicates that energy self-transfer between different macromolecular ligands was insignificant.

Fig. 7 shows a representative fluorescence bleaching curve of a FITC-IgE labeled cell. The bleaching curves contain two components. The amplitude of the large component (90–95%) varied with the amount of FITC conjugated antibody per cell and exhibited a bleaching time constant in the range of one second attributable to bleaching of fluorescein. The small component (5–10%, also observed for unlabeled cells) was due to background fluorescence and had a time constant in the range of 10–20 s.

The FRET efficiency $E$ was derived from the photobleaching time constants of the FITC component of the singly and doubly labeled cell samples according to Eq. 5. We measured routinely 15–30 single cells on each coverslip carrying single or double (IgE- or H10-Fab) labeled cells. Each series of measurements was repeated several times with freshly prepared coverslips. The results of the analyses, i.e., the FITC bleaching time constant $\tau$, standard deviations, and the FRET efficiency $E$, are also given in Table 1 along with the experimental details of each sample preparation ($Fc_\epsilon RI$ ligand, dye/protein ratio $n_{dye}$ of the mAb preparation used).

The data in Table 1 show the existence of a significant energy transfer of 0.075 ± 0.03 and 0.09 ± 0.02 between the IgE-$Fc_\epsilon RI$-complexes, for labeling ratios of 3.6 and 11, respectively. The measurements with the smaller and less conjugated H10-Fab fragments yielded lower FRET efficiencies: $E = 0.045 \pm 0.01$ for $n_a = 1.5$ and $E = 0.034 \pm 0.05$ for $n_a = 1.3$. From these results, we derived the ratios $r_E = 2.2$ and 1.7 for IgE ($n_a = 4$), and the H10-Fab ($n_a = 1.3$ and 1.5), respectively; for IgE, $n_a = 11$, and the H10-Fab, $n_a = 1.3$ and 1.5, $r_E = 2.6$ and 2.0. All ratios are greater than unity and thus, by comparison with our simulation, in line with the hypothesis of disperse noninteracting receptors. To illustrate this conclusion, we marked the experimental results in Fig. 6, *A* and *B* by arrows together with the respective standard deviations. It should be noted that Fig. 6 shows the ratios only for relatively small interaction energies $E_{int}$.producing receptor aggregation of up to 6% for $E_{int}$ of only 1.5 $kT$. Larger interaction energies causing a more extensive aggregation would lead to lower ratio values that are even less compatible with our data. Two of the experimentally established ratios (those that were derived from the measurements with the H10-Fab with $n_a = 1.3$) were not statistically significant, a result we attribute to an insufficient number of replicate determinations. However, these data still show that the energy transfer efficiency was smaller for H10-Fab labeled cells than for IgE labeled cells, a result compatible with that derived with the H10-Fab having $n_a = 1.5$.

## DISCUSSION

Energy transfer measurements provide information about the proximity of suitable donor and acceptor la-

**TABLE 1 Fluorescence resonance energy transfer efficiences between $Fc_\epsilon RI$ bound ligands on the surface of single RBL-2H3 cells**

| $n_{dye}$* | mAb‡ | $\tau$ (0.1 s)§ | $s$ (0.1 s)‖ | $n_{exp}$¶ | $E \cdot 100$** |
|---|---|---|---|---|---|
| 3.5 | I-F | 5.2 ± 0.12 | 0.7 | 35 | |
| 3.5, 3.6 | I-F, I-R | 5.7 ± 0.11 | 0.7 | 40 | 7.5 ± 3 |
| 1.1 | I-F | 4.6 ± 0.07 | 0.35 | 25 | |
| 1.1, 11 | I-F, I-R | 5.0 ± 0.08 | 0.4 | 25 | 8.1 ± 1.5 |
| 1.1 | I-F | 8.12 ± 0.15 | 0.75 | 25 | |
| 1.1, 11 | I-F, I-R | 9.0 ± 0.13 | 0.95 | 50 | 9.8 ± 2.1 |
| 1.2 | H-F | 3.8 ± 0.15 | 0.6 | 20 | |
| 1.2, 1.3 | H-F, H-R | 3.9 ± 0.17 | 0.8 | 20 | 3.4 ± 5 |
| 0.8 | H-F | 4.2 ± 0.06 | 0.65 | 120 | |
| 0.8, 1.5 | H-F, H-R | 4.4 ± 0.06 | 0.6 | 100 | 4.5 ± 1 |

* Dye/protein ratio.
‡ I-F, I-R: IgE-FITC, –TRITC; H-F, H-R: H10-Fab-FITC, –TRITC.
§ Bleaching time constant with standard error of the mean.
‖ Standard deviation of distribution.
¶ Number of single cell measurements.
** Energy transfer efficiency with standard deviation according to the Gaussian error propagation.

beled cell surface components. We addressed here the problem of the aggregation state of the $Fc_\epsilon RI$ on the surface of living individual RBL-2H3 cells by combining energy transfer measurements with a detailed theoretical analysis. In the experimental section of this report, two macromolecular ligands of different geometries covalently derivatized with fluorescent dyes were bound specifically to receptor molecules on the cell surface. IgE molecules were bound at their $Fc_\epsilon$ domains to the type I $Fc_\epsilon$-receptors on RBL-2H3 cells, whereas the Fab fragments of a monoclonal $Fc_\epsilon RI$ specific mAb, designated H10-Fab, were bound by their antigen binding sites. In the theoretical section, we presented a model describing our experimental system.

The final conclusion to be drawn from our analysis is that receptor aggregation should cause a higher energy transfer efficiency of cells labeled with H10-Fabs ($E_{H10}$) compared with cells labeled with IgE molecules ($E_{IgE}$). That is, the ratio $r_E = E_{Ige}/E_{H10}$ should equal or be smaller than unity. The results of our measurements, however, showed that IgE labeled cells exhibited a higher energy transfer efficiency than H10-Fab labeled cells for all values of $n_a$; i.e., $r_E$ was greater than unity (see Fig. 6). According to our theoretical analysis, this result implies that <5% of the total number of $Fc_\epsilon RI$ are at a distance of $\leq 5$ Å from each other on the surface of RBL-2H3 cells. This conclusion is in agreement with the results of Mendoza and Metzger (1976), Schlessinger et al. (1976), and McCloskey et al. (1984) with respect to the mobile fraction of $Fc_\epsilon RI$ deduced from lateral diffusion measurements but extends the findings to the significant fraction of surface $Fc_\epsilon RI$ found to be immobile. The combined theoretical and experimental approach to the analysis of the distribution of cell surface components is applicable to any cell system that displays a high surface density of the component in question and for which specific macromolecular ligands of different sizes are available.

We gratefully acknowledge many stimulating discussions with Prof. W. Dreybrodt and critical reading of the manuscript by G. Hummer. We thank Prof. Boseck for the supply of the Leitz MPV2, Mr. Lasch and Mr. Ankele for technical assistance, and Mr. Ankele for drawing Fig. 1.

Support of this research has been provided by generous grants from The Fritz Thyssen Foundation, Germany, and The Tobacco Research Council, USA. U. Kubitscheck gratefully acknowledges fellowships from the "Studienstiftung des Deutschen Volkes" and the MINERVA Foundation.

*Received for publication 21 August 1991 and in final form 26 August 1992.*

## REFERENCES

Barsumian, E. L., C. Isersky, M. G. Petrino, and R. P. Siraganian. 1981. IgE induces histamine release from rat basophilic leukemia cell lines: isolation of releasing and nonreleasing clones. *Eur. J. Immunol.* 11:317–323.

Blank, U., C. Ra, L. Miller, K. White, H. Metzger, and J.-P. Kinet. 1989. Complete structure and expression in transfected cells of high affinity IgE receptor. *Nature (Lond.).* 337:187–189.

Chan, S. S., D. J. Arndt-Jovin, and T. M. Jovin. 1979. Proximity of lectin receptors on the cell surface measured by fluorescence energy transfer in a flow system. *J. Histochem. Cytochem.* 27:56–62.

Dewey, T. G., and G. G. Hammes. 1980. Calculation of fluorescence resonance energy transfer on surfaces. *Biophys. J.* 32:1023–1035.

Edmundson, A. B., and K. R. Ely. 1986. Determination of the three dimensional structures of immunoglobulines. *In* Handbook of Experimental Immunology. Vol. 1. Immunochemistry. 4th ed. D. M. Weir, editor. Blackwell Scientific Publications, Oxford, UK. 15.1–15.23.

Erickson, J., W. P. Kane, R. G., B. Goldstein, D. Holowka, and B. Baird. 1986. Cross-linking of IgE-receptor complexes at the cell surface: a fluorescence method for studying the binding of monovalent and bivalent haptens to IgE. *Mol. Immunol.* 23:769–781.

Erickson, J. W., R. G., B. Posner, B. Goldstein, D. Holowka, and B. Baird. 1991. Bivalent ligand dissociation kinetics from receptor-bound immunoglobulin E: evidence for a time-dependent increase in ligand rebinding at the cell surface. *Biochemistry.* 30:2357–2363.

Fagan, M. H., and T. G. Dewey. 1986. Resonance energy transfer study of membrane-bound aggregates of the sarcoplasmic reticulum calcium ATPase. *J. Biol. Chem.* 261:3654–3660.

Förster, T. 1948. Zwischenmolekulare Energiewanderung und Fluoreszenz. *Ann. Phys.* 2:55–75.

Gill, G. N., P. J. Bertics, and J. B. Santon. 1987. Epidermal growth factor and its receptor. *Mol. Cell. Endocrinol.* 51:169–186.

Hasselbacher, C. A., T. L. Street, and T. G. Dewey. 1984. Resonance energy transfer as a monitor of membrane protein domain segregation: application to the aggregation of bacteriorhodopsin reconstituted into phospholipid vesicles. *Biochemistry.* 23:6445–6452.

Holowka, D., and B. Baird. 1983. Structural studies on the membrane bound immunoglobulin E-receptor complex. 2. Mapping of distances between sites on IgE and membrane surface. *Biochemistry.* 22:3475–3484.

Holowka, D., D. H. Conrad, and B. Baird. 1985. Structural mapping of membrane-bound immunoglobulin E-receptor complexes: use of monoclonal anti IgE antibodies to probe the conformation of receptor bound IgE. *Biochemistry.* 24:6260–6267.

James, F. 1972. Function minimization. *Proc. CERN-Computing Data Processing School, Pertisau, Austria.* 72–121.

Jovin, T. M., and D. J. Arndt-Jovin. 1989*a*. FRET microscopy: digital imaging of fluorescence resonance energy transfer. Application in cell biology. *In* Cell Structure and Function by Microspectrofluometry. E. Kohen, J. S. Ploem, and J. G. Hirschberg, editors. Academic Press, Orlando, FL. 99–117.

Jovin, T. M., and D. J. Arndt-Jovin. 1989*b*. Luminescence digital imaging microscopy. *Annu. Rev. Biophys. Biophys. Chem.* 18:271–308.

Kane, M. P., D. Holowka, and B. Baird. 1988. Crosslinking of IgE-receptor complexes by rigid antigens >200 Å in length triggers cellular degranulation. *J. Cell Biol.* 107:969–980.

Kubitscheck, U. 1990. Untersuchungen des transmembranen Signals zur Auslösung der Degranulation bei RBL-2H3-Zellen durch Messungen der Energieübertragung und Rotationsdiffusion. Ph.D. thesis. Universität Bremen, Germany.

Kubitscheck, U., M. Kircheis, R. Schweitzer-Stenner, W. Dreybrodt, T. M. Jovin, and I. Pecht. 1991. Fluorescence resonance energy transfer on single living cells: application to binding of monovalent haptens to cell-bound immunoglobulin E. *Biophys. J.* 60:307–318.

Lado, F. 1968. Equation of state of the hard-disk fluid from approximate integral equations. *J. Chem. Phys.* 49:3092–3096.

Liu, F. T., J. W. Bohn, E. L. Ferry, H. Yamamoto, C. A. Molinaro,

L. A. Sherman, N. R. Klinman, and D. H. Katz. 1980. Monoclonal dinitrophenyl-specific murine IgE antibody: preparation, isolation, and characterization. *J. Immunol.* 124:2728–2736.

McCloskey, M. A., Z. Y. Liu, and M. M. Poo. 1984. Lateral electromigration and diffusion of Fc epsilon receptors on rat basophilic leukemia cells: effects of IgE binding. *J. Cell Biol.* 99:778–787.

McQuarrie, D. A. 1976. Statistical Mechanics. Harper & Row, New York. 272–283.

Mendoza, G., and H. Metzger. 1976. Distribution and valency of the receptor for IgE on rodent mast cells and related tumor cells. *Nature (Lond.).* 264:548–550.

Metzger, H., G. Alcaraz, R. Hohman, J.-P. Kinet, V. Priluda, and R. Quarto. 1986. The receptor with high affinity for immunoglobulin E. *Annu. Rev. Immunol.* 4:419–470.

Myers, J. N., D. Holowka, and B. Baird. 1992. Rotational motion of monomeric and dimeric immunoglobulin E-receptor complexes. *Biochemistry.* 31:567–575.

Ortega, E., R. Schweitzer-Stenner, and I. Pecht. 1988. Possible orientational constraints determine secretory signals induced by aggregation of IgE receptors on mast cells. *EMBO (Eur. Mol. Biol. Organ.) J.* 7:4101–4109.

Pearson, L. T., S. I. Chan, B. A. Lewis, and D. M. Engelman. 1983. Pair distribution functions of bacteriorhodopsin and rhodopsin in model bilayers. *Biophys. J.* 43:167–174.

Pearson, L. T., J. Edelman, and S. I. Chan. 1984. Statistical mechanics of lipid membranes: protein correlation functions and lipid ordering. *Biophys. J.* 45:863–871.

Pecht, I., E. Ortega, and T. M. Jovin. 1991. Rotational dynamics of the receptor on mast cells monitored by specific monoclonal antibodies and IgE. *Biochemistry.* 30:3450–3458.

Perelson, A. 1978. Spatial distribution of surface immunoglobulin on B lymphocytes. *Exp. Cell Res.* 112:309–321.

Rudolph, A. K., P. D. Burrows, and M. R. Wahl. 1981. Thirteen hybridomas secreting hapten-specific immunoglobulin $\epsilon$ from mice with $Ig^a$ and $Ig^b$ heavy chain haplotype. *Eur. J. Immunol.* 11:527–529.

Ryan, T., J. N. Myers, D. Holowka, B. Baird, and W. W. Webb. 1988. Molecular crowding on the cell surface. *Science (Wash. DC).* 239:61–64.

Schlessinger, J., W. W. Webb, E. L. Elson, and H. Metzger. 1976. Lateral motion and valency of Fc receptors on rat peritoneal mast cells. *Nature (Lond.).* 264:550–552.

Schweitzer-Stenner, R., A. Licht, I. Luscher, and I. Pecht. 1987. Oligomerization and ring closure of immunoglobulin E class antibodies by divalent haptens. *Biochemistry.* 26:3602–3612.

Sims, P. J. 1984. Complement protein C9 labeled with fluorescein isothiocyanate can be used to monitor C9 polymerisation and formation of cytolytic membrane lesion. *Biochemistry.* 23:3248–3260.

Siraganian, P. R. 1988. Mast cells and basophils. *In* Inflammation: Basic Principles and Clinical Correlates. J. I. Gallin, M. Goldstein, and R. Snyderman, editors. Raven Press, New York. 513–542.

Sullivan, A. L., P. M. Grimley, and H. Metzger. 1971. Electron microscopic localization of immunoglobulin E on the surface membrane of human basophils. *J. Exp. Med.* 134:1403–1416.

Veatch, W., and L. Stryer. 1977. The dimeric nature of the gramicidin A transmembrane channel: conductance and fluorescence energy transfer studies on hybrid channels. *J. Mol. Biol.* 113:89–102.

Yarden, Y., and A. Ullrich. 1988. Growth factor receptor tyrosine kinases. *Annu. Rev. Biochem.* 57:443–478.

Zheng, Y., B. Shopes, D. Holowka, and B. Baird. 1992. Conformations of IgE bound to its receptor Fc$\epsilon$RI and in solution. *Biochemistry.* 31:7446–7456.

Zidovetzki, R., M. Bartholdi, D. Arndt-Jovin, and T. M. Jovin. 1986. Rotational dynamics of the Fc receptor for immunoglobulin E on histamine releasing rat basophilic leukemia cells. *Biochemistry.* 25:4397–4401.